

# PARAMETER SPACE BEYOND $10^{34}$

F. Zimmermann

CERN, Geneva, Switzerland

## Abstract

We review the beam parameters available for the LHC upgrade (intensities, betas, crossing angles, etc.), their constraints, interrelations, and the associated challenges, as well as the possible ranges that could be explored for each, and different luminosity optimization strategies.

Leveling of luminosity and/or of the beam-beam tune shift is likely to be important at the high-luminosity LHC. Formulae are presented for the ideal run time and average luminosity that can be achieved with and without two kinds of leveling schemes.

In particular, in this paper we demonstrate that the gain in luminosity from raising the beam intensity is much higher than from decreasing  $\beta^*$ , unless the latter is complemented by crab cavities or by smaller transverse beam emittance.

## INTRODUCTION

The parameter space for the LHC luminosity upgrade has first been charted in the 2001 LHC upgrade feasibility study [1]. It has later been refined and revisited in the frame of CARE-HHH [2], through several targeted workshops, e.g. [3,4,5,6], and, more recently, within the EuCARD-AccNet activity [7].

This paper reviews the parameters available, constraints and challenges for each, some relationships between these parameters, possible parameter ranges, and different optimization strategies, which either increase the beam intensity or decrease the interaction-point (IP) spot size.

The paper is structured as follows. The first part surveys the parameters and also recalls the original upgrade plan (the “ultimate” LHC) as well as several important constraints. Later, eight example scenarios are presented, covering the parameter space and illustrating the performance reach. The typical luminosity time evolution is presented, for various upgrade schemes. A third part of the paper addresses luminosity leveling, highlighting its merits and possibilities. We finally compute the impact of the turnaround time, of  $\beta^*$ , and of the bunch intensity on the average luminosity, and compare the luminosity gain expected from higher beam intensity with the one provided by tighter focusing, including, or not, additional measures.

## PARAMETERS

There are only a few relevant parameters:

- $\beta^*$  - the IP beta function;

- $\beta_x^*/\beta_y^*$  - the ratio of the IP horizontal and vertical IP beta functions\*,
- $\epsilon_N$  - the normalized transverse emittance;
- $N_b$  - the bunch intensity;
- $n_b$  – the number of bunches (or equivalently,  $s_b$ , the bunch spacing);
- the longitudinal bunch profile (“flat” versus “Gaussian” bunch shape);
- the number of interaction points (IPs); and
- $T_{ta}$  - the turn-around time.

## THE ORIGINAL PLAN – “PHASE 0”

The original plan for boosting the luminosity, as described e.g. in [1,9], was, or is, closely tied to the ultimate LHC parameters.

Figure 1 (left) shows that with the nominal LHC beam parameters, and the two protons beams colliding at 4 interaction points (in one of which off-center), the beam-beam tune footprint just fits into a square of width 0.01, which corresponds to the beam-beam limit experienced at the Sp $\bar{p}$ S collider. At a total beam-beam tune shift of 0.01 the betatron tune footprint can be accommodated in between resonances of order lower than or equal to 12. Reducing the number of IPs from 4 to 2, the beam-beam tune footprint shrinks by slightly more than 1/3 (Fig. 1 centre). This can be used to increase the bunch intensity until the tune footprint recovers its nominal size, at ultimate bunch intensity (Fig. 1 right). In these conditions, the ATLAS & CMS luminosity is a factor 2.3 higher than nominal, namely  $L \sim 2.3 \times 10^{34} \text{ cm}^{-2} \text{ s}^{-1}$  [1].

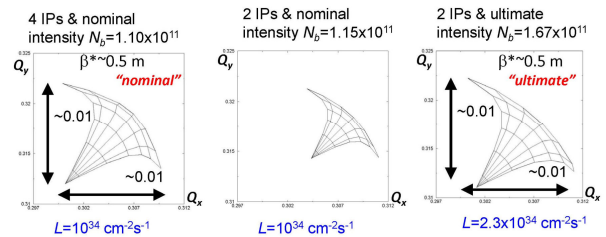


Figure 1: Beam-beam tune footprint up to  $6\sigma$  for the nominal LHC, as defined at the time, with collisions in four interaction points (left), with nominal collisions in 2 interaction points (centre), and with collisions in two interaction points at ultimate bunch intensity [1] [Courtesy H. Grote].

\*  $\beta_x^*/\beta_y^*$  ratios different from one are not further considered in the following, but they had been studied for the nominal LHC [ 8 ] and remain an interesting option for the future.

Alternatively, the same luminosity could be reached by reducing the fractional tune difference  $Q_y - Q_x$  from nominal 0.01 to 0.005, which would also allow increasing the bunch intensity to the ultimate value while maintaining collisions in all four IPs [9].

Moreover, increasing the crossing angle, to 340  $\mu\text{rad}$ , and the bunch length by a factor of 2, one could further raise the bunch charge to  $N_b = 2.6 \times 10^{11}$ , yielding  $L = 3.6 \times 10^{34} \text{ cm}^{-2} \text{ s}^{-1}$  at  $\beta^* = 0.5 \text{ m}$  [1].

## BUNCH PATTERNS AND LHCb

Only two or three types of bunch pattern are considered for the upgrade: the nominal 25-ns bunch spacing with ultimate or slightly higher bunch intensity, or 50-ns spacing with about twice this intensity per bunch.

For Super-LHC, the upgraded LHCb detector requires luminosities equal to a few percent of the peak luminosity in IP1 and 5 [10].

It is not easy to deliver this LHCb luminosity for the 25-ns bunch pattern, without losing potential luminosity in ATLAS and CMS in view of the additional tune-shift contribution from LHCb. One possibility is arranging for “late collisions” with  $\beta^* \sim 3 \text{ m}$ . This might, however, not be compatible with all the luminosity-leveling schemes [11,12].

In the 50-ns pattern one could add lower-intensity “satellite” bunches 25 ns behind the main bunches, so that at LHCb the main bunches would collide with the satellite bunches [11,12]. The luminosity in LHCb would be determined by the charge of the satellites. Alternatively, one could also arrange for the satellite and main bunches to collide in ALICE. Two advantages of the scheme with 50-ns spacing are:

- insignificant electron cloud (which remains true even in the presence of satellites; see later); and
- almost complete transparency of LHCb (or ALICE) collisions for ATLAS and CMS.

Figure 2 illustrates the various bunch patterns considered for the LHC upgrade.

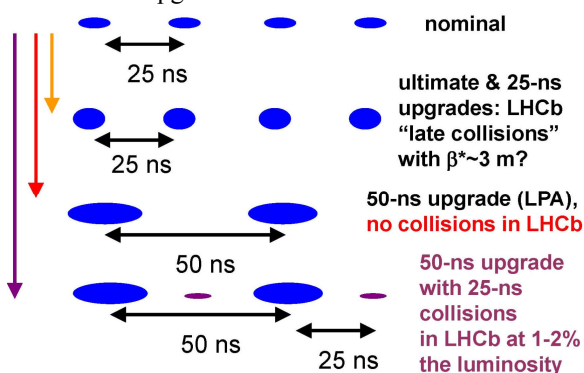


Figure 2: Bunch patterns for the LHC luminosity upgrade with and without collisions in (S)LHCb.

## CONSTRAINTS

The most important parameter constraints are as follows:

- the total beam-beam tune shift should not exceed 0.01, based on the SPS p-pbar experience;

- the long-range beam-beam effect calls for a crossing angle larger than  $\geq 9\sigma^*$  (i.e. more than  $9\sigma$  separation at the majority of the parasitic beam-beam encounters [13]);
- the arc cooling capacity is restricted by both global & local limitations; one important global limit arises from the fact that the arc cooling is presently shared with the interaction region magnets, which at high luminosity receive a lot of heat from collision debris; independent cryo plants for the interaction regions would much improve this limit; the heat load in the arcs is the sum of contributions from synchrotron radiation, image currents (mostly resistive wall), and electron cloud including photo-electrons;
- the interaction layout and optics define the minimum  $\beta^*$ ;
- the event pile up in the detectors should be less than 150-300 events per crossing, the exact limit depending on the details of the detector upgrade and the physics scenario, and
- the luminosity lifetime should not be too short; requiring a value above 5 h appears reasonable.

## CROSSING ANGLE

Controlling the effect of the large number of parasitic collisions (120) in LHC requires a crossing angle, which must increase with the beam intensity and in particular scales as  $1/\beta^{*1/2}$ . The direct effect of the crossing angle on the overlap of the colliding bunches and on the luminosity is characterized by the so-called Piwinski angle  $\phi$  and the geometric luminosity reduction factor  $R_\phi$ ,

$$R_\phi = \frac{1}{\sqrt{1 + \phi^2}}; \quad \phi \equiv \frac{\theta_c \sigma_z}{2\sigma_x^*}, \quad (1)$$

where  $\theta_c$  denotes the full crossing angle,  $\sigma_z$  the rms bunch length and  $\sigma_x^*$  the transverse rms IP beam size (in the plane of crossing).

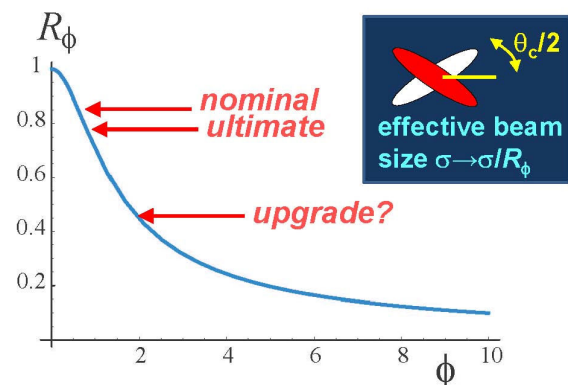


Figure 3: Geometric reduction factor as a function of the Piwinski angle, and operating points for nominal, ultimate, and a typical upgraded LHC.

Figure 3 shows the values of these two parameters for collisions in the nominal and the ultimate LHC and for a typical upgrade scenario. The insert illustrates the origin

of the luminosity loss. While for the nominal LHC the loss is less than 20%, it approaches 60% for an upgrade at  $\phi \sim 2$  (or, in other words, without this factor the upgrade luminosity could be 2.5 times higher!).

The accessible range of crossing angles depends on the design of the final quadrupole triplet (aperture, gradient, length) and on  $\beta^*$ . The nominal crossing angle is 285  $\mu\text{rad}$ ; it rises to 315  $\mu\text{rad}$  for the ultimate LHC. Crossing angles up to  $\sim 410$   $\mu\text{rad}$  are considered for the IR “phase 1” [14] and up to about 500  $\mu\text{rad}$  for some “phase 2” scenarios.

### BEAM-BEAM TUNE SHIFT, PIWINSKI ANGLE, AND LUMINOSITY

The total (horizontal or vertical) beam-beam tune shift for the case of two interaction points with alternating horizontal and vertical crossing is [15]

$$(2) \quad \Delta Q_{bb} = \frac{N_b r_p}{\gamma \varepsilon} \frac{1}{2\pi} \frac{1}{\sqrt{1 + \phi_{piw}^2}} \frac{1}{F_{profile}}$$

where the factor  $\gamma \varepsilon$  represents the normalized emittance,  $N_b$  is the number of particles per bunch,  $r_p$  the classical proton radius, and  $F_{profile}$  a form factor, equal to 1 for a longitudinally Gaussian bunch shape and  $\sqrt{2}$  for a flat profile.

According to (2) the beam-beam tune shift decreases as a function of crossing angle exactly with the same factor  $R_\phi$  as the luminosity (compare Eq. (1)). In addition, the form factor  $F_{profile}$  expresses the fact that a longitudinally “flat” profile is preferred since the maximum beam-beam tune shift depends primarily on the peak charge density.

The luminosity can be written in the following two alternative ways [15]

$$(3) \quad L = \frac{1}{4\pi} f_{rev} n_b \gamma \frac{1}{\beta^* (\gamma \varepsilon)} N_b^2 \frac{1}{\sqrt{1 + \phi_{piw}^2}}$$

$$= \frac{\pi}{r_p^2} f_{rev} n_b \gamma \frac{(\gamma \varepsilon)}{\beta^*} \Delta Q_{bb}^2 F_{profile}^2 \sqrt{1 + \phi_{piw}^2}$$

where the first equation is useful below the beam-beam limit and the second equation guides the luminosity optimization at the beam-beam limit when  $\Delta Q_{bb}$  has reached a constant value. In the former case, one aims to minimize the Piwinski angle  $\phi$ , whereas in the second case, i.e. at the beam-beam limit, the luminosity can be further increased by raising  $\phi$  and, e.g.,  $N_b$  or  $\varepsilon$  at the same time. From (2) and (3) one can also deduce that for the same bunch charge  $N_b$  and the same beam-beam tune shift  $\Delta Q_{bb}$ , the luminosity of a uniform (or ‘flat’) longitudinal distribution is exactly  $\sqrt{2}$  times higher than for a Gaussian bunch profile [16].

Based on the above relationships, a number of luminosity optimization strategies have been proposed for the LHC upgrade [3,4,5,6,17]:

- increase  $N_b$  together with  $\varepsilon$ , e.g. via controlled  $\varepsilon$  blow up at top energy (“Big Emittance”);

- increase  $N_b$  with  $1/R_f$  & “flat” bunch  $F_{profile} \sim 1.4$  (“Large Piwinski Angle - LPA”);
- vary  $\varepsilon$  as  $1/R_\phi$  (“Low Emittance - LE”); or
- aim for  $R_\phi \sim 1$  at the IP and minimize  $\beta^*$  (e.g. “Crab Crossing - CC” and “Early Separation - ES” schemes).

### BEAM-BEAM TUNE SHIFT LIMIT & THE CROSSING ANGLE

Several of our optimization strategies, described above, assume that the “beam-beam limit” is uniquely characterized by a maximum value of the beam-beam tune shift  $\Delta Q_{tot}$ , and that this limiting value itself does not depend on the crossing angle  $\theta_c$ . In lepton colliders this assumption is known to be not fully valid: in various e+e- colliders the finite crossing angle has lowered the maximum value of the beam-beam limit which could be achieved, e.g. at DORIS-I, and KEKB. One reason for the observed tune-shift degradation is the excitation of synchro-betatron resonances by a non-zero crossing angle. At KEKB the potential increase in the maximum beam-beam tune shift for zero crossing angle has in fact been the main motivation for installing crab cavities.

For colliding hadron beams, we are aware of only a single experiment concerning the effect of a crossing angle on the beam-beam limit, which was performed at the SPS collider about two decades ago [18]. The main results of this experiment are shown in Fig. 4. Only a faint additional beam-beam effect has been observed in the loss rates for the largest  $\phi$  examined ( $\sim 0.7$ ). However, the  $\phi$  values explored in the historical SPS experiment did not extend to the  $\phi$  range between 1 and 3, which is being considered for the LHC upgrade.

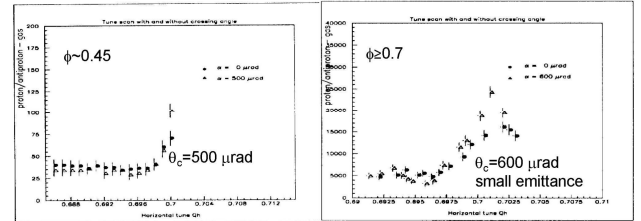


Figure 4: Experimental background rates in the SppS collider as a function of the horizontal tune with and without a crossing angle, for a Piwinski angle  $\phi$  around 0.45 (left) and 0.7 (right) [18].

### CRAB CROSSING

Crab crossing was first proposed for linear [19] and then for circular e+e- colliders [20] in 1988 and 89, respectively. Since 2007, crab cavities are in operation at KEKB. The principle of the crab crossing is illustrated in Fig. 5. A transversely deflecting RF “crab cavity” deflects the head and tail of each passing bunch in opposite directions so that the beam-beam collision becomes effectively “head on” for the luminosity and for the tune shift. Whereas the overlap and the field are restored, the bunch centroids still cross at a finite angle which allows

for easy separation, and minimizes the effect of parasitic beam-beam encounters.

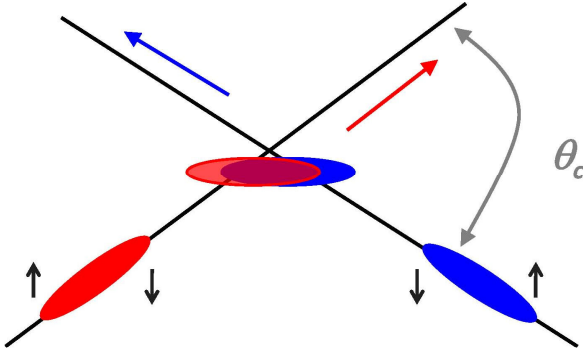


Figure 5: Schematic of crab crossing.

The potential merits of crab cavities for the LHC [21] include a higher geometric luminosity, the possibility easy luminosity leveling, as well as – in view of the above considerations – a potentially higher beam-beam tune shift limit.

### LARGE PIWINSKI ANGLE

Optimizing the LHC luminosity at the beam-beam limit by collisions with a Large Piwinski Angle (LPA), e.g.  $\theta_c \sigma_z \gg 2\sigma_x^*$ , and longer, longitudinally flat, and intense bunches was first proposed in [1,15]. The concept is based on Eqs. (2) and (3). Figure 6 presents a rough schematic of LPA collisions. The large value of  $\phi$  and the flat profile both translate into a reduced tune shift, and the resulting potential for higher bunch charge, which is taken advantage of in the LPA schemes proposed for the LHC. To restrict the heat load from electron cloud in the cold LHC arcs, the standard LPA scenario for LHC considers 50 ns spacing.

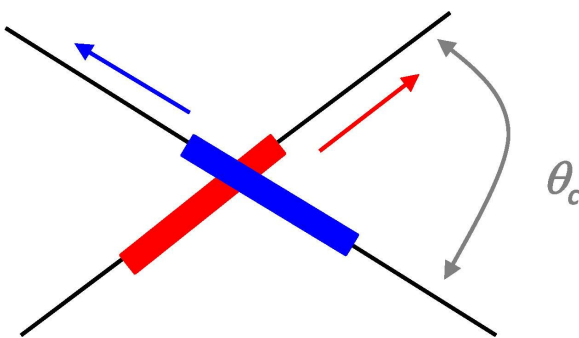


Figure 6: Schematic of the “Large Piwinski Angle” (LPA) collision scheme.

### BUNCH INTENSITY

The beam-beam tune shift due to the primary collisions introduces a limit on the bunch intensity through (2). This is a fundamental limit for crab cavities without leveling. Raising the number of protons per bunch,  $N_b$ , beyond the ultimate bunch intensity of  $1.7 \times 10^{11}$  requires either a large Piwinski angle or a large emittance. In certain scenarios restricting the beam-beam tune shift from the primary

collision points requires even larger crossing angles than what would be needed for preventing harmful long-range beam-beam effects due to the parasitic encounters.

Another severe limit for the bunch intensity is imposed by the arc cooling capacity. The next section discusses this in more detail.

Other, less fundamental limits on the bunch intensity may come from the injectors, collimation, machine protection, radiofrequency system, etc.

### ARC COOLING & HEAT LOAD

The cooling capacity for the cold LHC arcs is limited both globally, by the cooling power of the cryo plants, which must also cool the interaction region quadrupoles – at high luminosity subjected to large heat from collision debris –, and locally, by the hydraulic impedance of the beam-screen cooling loops [22–24]. In the LHC arcs proper, synchrotron radiation, image currents (together with the resistive wall impedance) and electron cloud are the main sources of heat load. The heat from synchrotron radiation and impedance can be fairly accurately calculated [23,24]. The heat load from electron cloud is obtained from simulations [25]. The most optimistic simulations consider a maximum secondary emission yield below 1.3, where beam-induced multipacting is largely absent, and where the remaining electron-induced heating is dominated by the accelerated primary photoelectrons.

Figures 7 and 8 compare, for a bunch spacing of 25 ns and 50 ns, respectively (and with different IP beta functions), the residual cooling capacity available and the simulated heat load from the electron cloud. Here, the residual cooling capacity is calculated by subtracting from the global limit the equivalent cooling power required for the interaction region (depending on the luminosity), and the computed heating from synchrotron radiation and image currents, and from the local limit only the latter two arc contributions, and then taking the minimum value of the remaining global and local cooling capacities so obtained.

Both figures, 17 and 18, demonstrate that in order to reach any decent bunch intensity at high luminosity (actually the first is a precondition for the latter), separate dedicated cryo plants are needed for the interaction regions. More specifically, Fig. 7 shows that for 25-ns bunch spacing, going above  $N_b = 1.7 \times 10^{11}$  protons per bunch at nominal  $\beta^*$  requires dedicated IR cryo plants; if such plants are installed the “hard” intensity limit becomes  $N_b \sim 2.3 \times 10^{11}$ . From Fig. 8, for 50-ns bunch spacing, dedicated IR cryo plants are required at bunch intensities above  $N_b = 2.3 \times 10^{11}$  with an upgraded  $\beta^* \sim 0.25$  m; again assuming a separate IR cooling, the hard limit on the bunch intensity is pushed to  $N_b \sim 5 \times 10^{11}$ .

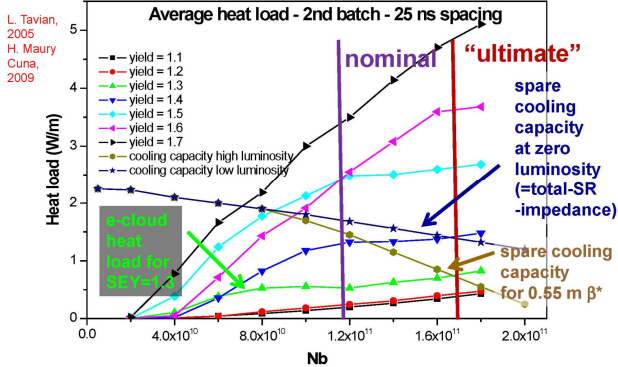


Figure 7: Residual cooling capacity for electron cloud per aperture and per meter at low and high luminosity at  $\beta^*=0.55$  m (or with and without dedicated IR cryo plants) as a function of bunch intensity [22-24] together with the electron cloud heat load simulated for various values of the maximum secondary emission yield and 25-ns bunch spacing, with a Gaussian bunch profile [25].

Figure 9 presents simulated heat loads for the 50-ns bunch spacing of the standard LPA scheme with and without dedicated LHCb satellite bunches interleaved at a distance of 25 ns from the main bunches [25]. The satellite bunch intensity is decreased inversely proportional to the main bunch intensity in order to provide a constant target luminosity in LHCb (determined by collisions between main bunches and satellites). The figure illustrates that the heat load including the “LHCb satellite” does not show a fully monotonic dependence on the main bunch intensity, which is consistent with earlier studies of other types of LHC satellite bunches [26,27], but that the additional smaller bunches only marginally increase the (low) 50-ns heat load.

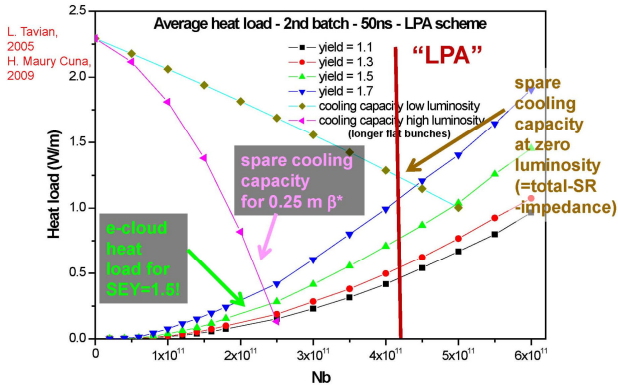


Figure 8: Residual cooling capacity for electron cloud per aperture and per meter at low and high luminosity (or with and without dedicated IR cryo plants) for a bunch spacing of 50 ns and  $\beta^*=0.25$  m as a function of bunch intensity [22-24] together with the electron cloud heat load simulated for various values of the maximum secondary emission yield. A longitudinally flat bunch shape is assumed (LPA scenario) [25].

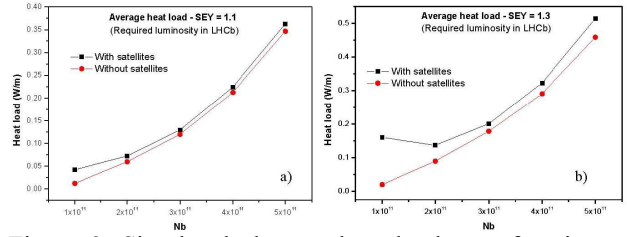


Figure 9: Simulated electron heat load as a function of main bunch intensity for 50 ns bunch spacing with (black) and without LHCb satellite bunches (red) for two different values of the maximum secondary emission yield ( $\delta_{\max}=1.1$  – left, and  $\delta_{\max}=1.3$  – right) [25]. In this simulation, the satellite bunch intensity has been varied as the inverse of main-bunch intensity, as  $N_{b,\text{sat}} \sim 1.1 \times 10^{10} \times 5 \times 10^{11} / N_{b,\text{main}}$ , in order to yield a constant target luminosity of about  $2 \times 10^{33} \text{ cm}^{-2}\text{s}^{-1}$  in (S)LHCb.

## IP BETA FUNCTION

The nominal LHC IP beta function is 0.55 m. For the ultimate LHC a beta function of 0.5 m has been retained, e.g. [28]. The proposed “phase-1” IR upgrade with larger aperture Nb-Ti quadrupoles allows for beta functions between 0.25 m and 0.4 m [14,29]. For a later phase-2 upgrade based on Nb<sub>3</sub>Sn quadrupoles, beta functions between 0.14 and 0.22 m have been considered at the present value of  $l^*$  equal to 23 m (free length between the last quadrupole and the IP). The value of 0.14 m is a hard limit from the arc-sextupole strength required by the linear chromatic correction. For a reduced  $l^*$  of about 13 m, an even smaller IP beta functions close to 0.1 m could be envisioned [30].

In addition to the linear chromaticity, other “softer” limitations arise from the physical aperture in the matching sections, and from the additional sextupole strength required for the correction of the off-momentum beta beating in the two cleaning insertions.

It may be worth noting that some past attempts at designing a local chromatic correction scheme, which would not rely on the arc sextupoles and not generate a large off-momentum beta beating, have not been successful, but that this approach could be reconsidered.

## EVENT PILE UP

One major concern is the event pile up in the detectors, LHC studies in the first half of the 1980s had constrained the number of events per crossing to less than 1. The nominal LHC parameters imply about 19 inelastic scattering events per bunch crossing, assuming an inelastic cross section of about 60 mbarn. A 10 times higher luminosity for the same number of bunches translates into about 200 events per crossing, necessitating an upgrade of the present detectors.

The number of events per crossing is equal to the product of the relevant inelastic cross section and the luminosity divided by the bunch collision rate, where the

bunch collision rate is given by the product of the number of bunches per beam and the revolution frequency.

## LUMINOSITY DECAY AND LIFETIME

For the upgraded LHC a fast decay of beam intensity and luminosity is expected (with a typical time scale of a few hours), which is dominated by proton burn off in proton-proton collision. Contributions from intrabeam scattering and from gas scattering can be considered negligible in comparison. Under these conditions, the luminosity decay will not be exponential, but purely algebraic, and of the form [31]

$$L(t) = \frac{\hat{L}}{(1 + t/\tau_{\text{eff}})^2} \quad (4)$$

where  $\tau_{\text{eff}}$  denotes the effective initial beam lifetime

$$\tau_{\text{eff}} = \frac{N_b n_b}{n_{\text{IP}} \hat{L} \sigma_{\text{tot}}} \quad (5)$$

and we recognize the number of protons per bunch  $N_b$ , the number of bunches per beam  $n_b$ , the number of IPs, the initial peak luminosity  $\hat{L}$  and the total scattering cross section  $\sigma_{\text{tot}}$ .

The beam and luminosity lifetimes are proportional to the total beam intensity and inversely proportional to the luminosity. An LHC luminosity upgrade implies shorter luminosity lifetimes unless the beam intensity is increased simultaneously. Or, in other words, for a given peak luminosity, the luminosity lifetime depends only on the total beam current (at least in the absence of “leveling”).

The beam lifetime is related to the total cross section. For the LHC centre-of-mass energy the total cross section is quite well known from cosmic ray experiments; see Fig. 10. Extrapolation of the inelastic cross section, relevant for the event pile up, were experimental data exist only at much lower energies, to the LHC appears to be more uncertain.

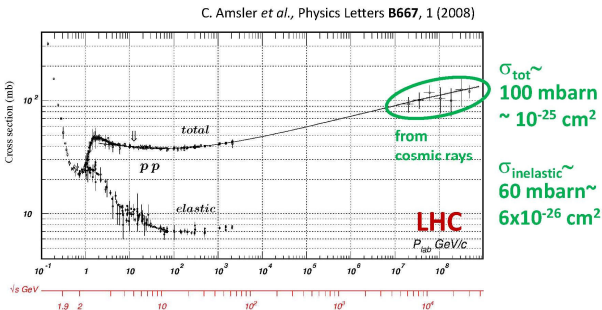


Figure 10: Total and elastic cross sections for  $pp$  collisions as a function of laboratory beam momentum and total center-of-mass energy. Corresponding computer-readable data files may be found at <http://pdg.lbl.gov/current/xsect/>. (Courtesy of the COMPAS group, IHEP, Protvino, August 2005) [32].

## EXAMPLE SCENARIOS

The parameter space available is spanned by a number of scenarios, characterized as follows:

- (1) “nominal LHC”:  $N_b=1.15 \times 10^{11}$ ,  $\beta^*=0.55$  m,  $\theta_c=285$   $\mu$ rad, and 25-ns bunch spacing;
- (2) “nominal\*”:  $N_b=1.7 \times 10^{11}$ ,  $\beta^*=0.55$  m,  $\theta_c=285$   $\mu$ rad, and 50 ns bunch spacing;
- (3) “ultimate LHC”:  $N_b=1.7 \times 10^{11}$ ,  $\beta^*=0.50$  m,  $\theta_c=315$   $\mu$ rad, and 25-ns bunch spacing;
- (4) “phase 1+” with maximum intensity permitted by beam-screen cooling loops and minimum  $\beta^*$  from phase-1 upgrade:  $N_b=2.3 \times 10^{11}$ ,  $\beta^*=0.30$  m,  $\theta_c=348$  mrad, and 25-ns bunch spacing;
- (5) “phase 1 with crab”, with an intensity slightly below ultimate and crab crossing:  $N_b=1.6 \times 10^{11}$ ,  $\beta^*=0.30$  m ( $\theta_c=348$   $\mu$ rad), and 25-ns bunch spacing;
- (6) “phase 2+” with maximum intensity permitted by beam screen cooling loop and minimum conceivable  $\beta^*$ :  $N_b=2.3 \times 10^{11}$ ,  $\beta^*=0.14$  m,  $\theta_c=509$   $\mu$ rad, and 25-ns bunch spacing;
- (7) “phase 2 with crab” again with an intensity slightly below ultimate,  $N_b=1.6 \times 10^{11}$ ,  $\beta^*=0.14$  m ( $\theta_c=509$   $\mu$ rad), and 25-ns bunch spacing [we also consider this same case without crab cavity to reveal the merit of the latter];
- (8) 50-ns “LPA” scenario, with 50-ns bunch spacing, and flat long bunches:  $N_b=4.2 \times 10^{11}$ ,  $\beta^*=0.25$  m,  $\theta_c=381$   $\mu$ rad; and
- (9) 25-ns “LPA” scenario, with 25-ns bunch spacing, and flat long bunches:  $N_b=2.6 \times 10^{11}$ ,  $\beta^*=0.50$  m,  $\theta_c=339$   $\mu$ rad.

Table 1 compiles numerous parameters for the above eight scenarios, including peak luminosity, beam current, maximum number of events per crossing, the individual contributions to the arc heat load, optimum run time and average luminosity for two different values of turn-around time (2 and 10 h), and, in the last row, the annual luminosity calculated assuming 60% machine availability for physics, an average 5-h turn-around time, and 200 days total run time per year.

Optimum run time and average luminosities have been calculated using the expected algebraic decay (4). At other occasions, estimates have been based on an exponential approximation to the algebraic shape of the form [33]

$$L(t) \approx \hat{L} \exp(-1.54t/\tau_{\text{eff}}) \quad (6)$$

Figure 11 illustrates the quality of this approximation. In the time interval between 0 and  $\tau_{\text{eff}}$ , the exponential approximation (6) looks fairly good. However, the merit of this approximation is not clear, as neither the consumption in collision nor intrabeam scattering, or gas scattering, lead to exponential luminosity decay. For calculating optimum run times and average luminosities without leveling, this paper only considers the algebraic luminosity decrease (4).

Table 1: Example upgrade parameters.

parameter	symbol	nom.	nom.*	ult.	$\beta^*=30$ cm, HI	$\beta^*=30$ ,cm , CC	$\beta^*=14$ , cm HI	$\beta^*=14$ cm, CC	LPA – 25	LPA – 50
transverse emittance	$\varepsilon$ [ $\mu\text{m}$ ]	3.75	3.75	3.75	3.75	3.75	3.75	3.75	3.75	3.75
protons per bunch	$N_b$ [ $10^{11}$ ]	1.15	1.7	1.7	2.3	1.6	2.3	1.6	2.6	4.2
bunch spacing	$\Delta t$ [ns]	25	50	25	25	25	25	25	25	50
beam current	$I$ [A]	0.58	0.43	0.86	1.16	0.81	1.16	0.81	1.32	1.06
longitudinal profile		Gauss	Gauss	Gauss	Gauss	Gauss	Gauss	Gauss	Flat	Flat
rms bunch length	$\sigma_z$ [cm]	7.55	7.55	7.55	7.55	7.55	7.55	7.55	11.8	11.8
beta* at IP1&5	$\beta^*$ [m]	0.55	0.55	0.5	0.30	0.30	0.14	0.14	0.50	0.25
full crossing angle	$\theta_c$ [ $\mu\text{rad}$ ]	285	285	315	348	(348)	509	(509)	339	381
Piwiński parameter	$\phi = \theta_c \sigma_z / (2^* \sigma_x^*)$	0.65	0.65	0.75	1.1	0.0	2.3	0.0	2.0	2.0
tune shift	$\Delta Q_{tot}$	0.009	0.0136	0.009	0.01	0.01	0.006	0.01	0.01	0.01
peak luminosity	$L$ [ $10^{34} \text{ cm}^{-2}\text{s}^{-1}$ ]	1	1.1	2.3	5.9	4.0	7.5	7.9	4.0	7.4
peak events per #ing		19	40	44	111	76	142	150	75	280
initial lumi lifetime	$\tau_L$ [h]	23	16	15	7.7	7.8	6.0	4.0	12.4	5.3
effective luminosity ( $T_{\text{turnaround}}=10 \text{ h}$ )	$L_{\text{eff}}$ [ $10^{34} \text{ cm}^{-2}\text{s}^{-1}$ ]	0.45	0.43	0.90	1.8	1.2	2.0	1.7	1.5	1.9
	$T_{\text{run,opt}}$ [h]	21.5	17.7	17.2	12.4	12.5	11.0	8.9	16.0	10.5
effective luminosity ( $T_{\text{turnaround}}=2 \text{ h}$ )	$L_{\text{eff}}$ [ $10^{34} \text{ cm}^{-2}\text{s}^{-1}$ ]	0.67	0.68	1.41	3.2	2.2	3.8	3.5	2.4	3.6
	$T_{\text{run,opt}}$ [h]	9.6	7.9	7.7	5.5	5.6	4.9	4.0	7.2	4.7
e-c heat SEY=1.3	$P$ [W/m]	0.4	0.1	0.6	1.3	0.7	1.3	0.7	1.4	0.8
SR heat 4.6-20 K	$P_{\text{SR}}$ [W/m]	0.17	0.13	0.25	0.34	0.24	0.34	0.24	0.38	0.31
image current heat	$P_{\text{IC}}$ [W/m]	0.15	0.17	0.33	0.60	0.29	0.60	0.29	0.39	0.51
gas-s. 100 h $\tau_b$	$P_{\text{gas}}$ [W/m]	0.04	0.03	0.06	0.08	0.05	0.08	0.05	0.09	0.07
luminous region	$\sigma_l$ [cm]	4.5	4.5	4.3	3.7	5.3	2.2	5.3	5.2	3.8
annual luminosity	$L_{\text{im}}$ [ $\text{fb}^{-1}$ ]	57	56	116	245	169	286	253	198	274

normalized luminosity

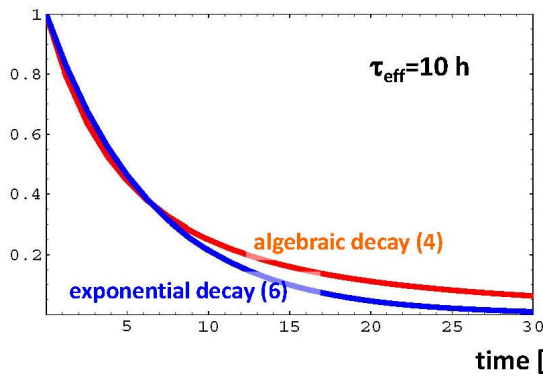


Figure 11: Comparison of the algebraic luminosity decay (4) with an exponential approximation for  $\tau_{\text{eff}}=10 \text{ h}$ .

The turn-around time is defined as the time interval between the end of one (data-taking) physics run and the start of the next. It includes the ramping down of the magnets, pre-cycling, injection, acceleration, and squeeze.

The LHC Design Report and other sources indicate a minimum LHC turn-around time of about 4300 seconds (1.2 h) [34,35]. This Chamonix workshop has clarified that the minimum actually achievable turn-around time is three times longer, i.e. 3 hours [33]. Moreover, from experience at other similar machines (Tevatron, HERA, and RHIC) it is expected that the actual average turn-around time in operation will be about three times the minimum value [36], which would then translate to about 10 h for the LHC.

Figure 12 illustrates the luminosity time evolution expected for six of the above scenarios and Fig. 13 allows a closer view at four of them, corresponding to some of the “phase-2” or LPA scenarios. From Fig. 13 it is evident that the scenario with  $\beta^*=14 \text{ cm}$  and  $N_b=2.3 \times 10^{11}$  (phase 1+) has a very similar performance to the one with  $\beta^*=14 \text{ cm}$ , the lower intensity of  $N_b \sim 1.6 \times 10^{11}$  and crab cavities (phase 1 with crab), and also to the LPA scheme with  $\beta^*=25 \text{ cm}$ ,  $N_b=4.2 \times 10^{11}$  and 50-ns spacing (LPA-50).

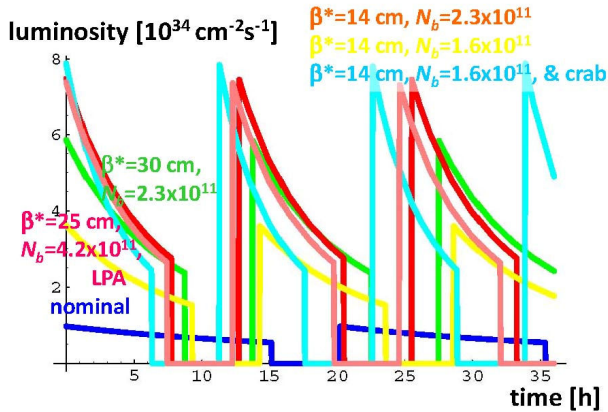


Figure 12: Luminosity evolution as a function of time during physics operation for several upgrade scenarios, and for the nominal LHC, with a turnaround time of 5 h.

Figure 14 shows the corresponding time evolution for the number of events per bunch crossing. Here, all scenarios imply peak rates of 100-150 events per crossing, except for the 50-ns LPA scheme, where this rate is close to 300. The number of events per may not be the only relevant quantity. E.g. there might be several sub-detectors integrating over more than one bunch crossing.

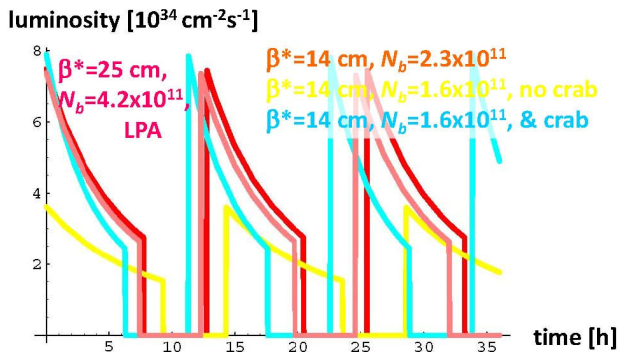


Figure 13: Luminosity evolution as a function of time during physics operation for some selected phase-2 and LPA upgrade scenarios, with a turnaround time of 5 h.

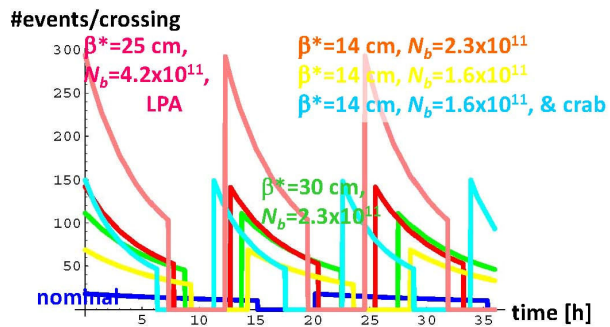


Figure 14: Number of events per crossing as a function of time during physics operation for several upgrade scenarios, and the nominal LHC (all with 5 h turnaround).

## LUMINOSITY LEVELING

The term “luminosity leveling” designates a controlled change of  $\theta_c$ ,  $\beta^*$  or  $\sigma_z$  during the store in order to reduce the maximum event pile up and the peak power deposition in the interaction region magnets, as well as, for some of the leveling schemes, also in order to maximize the integrated luminosity. The radiation damping from synchrotron radiation already naturally provides some kind of leveling by reducing the beam size during a store, though the LHC transverse radiation damping time of 52 h at 7 TeV beam energy is much longer than the luminosity lifetimes of between 4 and 12 h expected for the high-luminosity LHC (see Table 1) [37].

Leveling by squeezing  $\beta^*$  in physics had initially been proposed for the LHC heavy ion programme, with the aim to maximize the physics output without exceeding the quench threshold of the most sensitive SC magnets in the dispersion suppressors [38]. It is possible that luminosity leveling in the LHC will first be tested in heavy-ion collisions.

Luminosity leveling for LHC proton collisions, by varying either  $\beta^*$  or the bunch length, was first suggested at a PAF/POFPA meeting in 2007 [39]. The idea of leveling with the crossing angle using dipole magnets was introduced by J.-P. Koutchouk and G. Sterbini for the so-called early-separation scheme (with dipole magnets embedded in the particle-physics detector) [40,41]. Leveling with the crossing angle could alternatively be realized by varying the crab-cavity voltage [42].

Leveling with the crossing angle has two advantages compared with leveling through the IP beta function: namely (1) it offers the possibility to actually increase the average luminosity and (2) it is operationally simpler. In particular, as indicated above, leveling with the crossing angle is a natural option for the so-called early separation schemes and for crab cavities.

Two leveling strategies can be identified – an original one which is keeping the luminosity constant and another one where the beam-beam tune shift is held constant during the store. The first scheme has been discussed over the last couple of years. If the luminosity is held constant by changing the crossing angle, the tune shift increases during the store. This is the motivation for the second scheme, which is newly proposed in this paper.

Table 2 compiles analytical formulae for the luminosity time evolution, the optimum run time, and the time-averaged luminosity, without leveling and with either of the two aforementioned leveling schemes. It is interesting to notice that the second leveling scheme, which maintains a constant beam-beam tune shift during the store leads to an exponential decay of both beam current and of luminosity, with an identical time constant (!), and not with a factor 2 shorter decay constant for the luminosity as one would expect without leveling, and neither with a factor 1.54 difference as in (6).

Figure 15 presents example time evolutions of luminosity and beam-beam tune shift for the scenario



called phase 2+ (the seventh column in Table 1) without any leveling and with either of the two leveling schemes. For the same scenario, Table 3 illustrates the merit of leveling in numbers, considering different values of initial luminosity and initial beam-beam tune shift, varied via the initial crossing angle. Comparing the second and the fifth column, leveling here increases the run time by 50% and at the same time it raises the average luminosity by some 15%, both of which is desirable. Table 4 shows a similar comparison for the LPA scenario with 50 ns bunch spacing. Comparing the second and fourth columns, leveling increases the optimum run time by a factor of more than 3, from 7 to 23 h, and it reduces the peak pile up from about 280 to 170 events per crossing, at the expense of a 20% loss in luminosity. Other leveling choices are possible. For example, in the third column, the average luminosity is almost the same as without leveling, while the peak pile up is still reduced to about 170, but the run time is only 6 h in this case.

Table 2: Analytical expressions for the time evolution of luminosity and beam current, for the optimum run time, and for the average luminosity, with and without leveling, and considering two different leveling schemes.

	w/o leveling	$L=\text{const}$	$\Delta Q_{\text{bb}}=\text{const}$
luminosity evolution	$L(t) = \frac{\hat{L}}{(1+t/\tau_{\text{eff}})^2}$	$L = L_0 \approx \text{const}$	$L(t) = \hat{L} \exp(-t/\tau_{\text{eff}})$
beam current evolution	$N(t) = \frac{N_0}{(1+t/\tau_{\text{eff}})}$	$N = N_0 - \frac{N_0}{\tau_{\text{eff}}} t$	$N(t) = N(0) \exp(-t/\tau_{\text{eff}})$
optimum run time	$T_{\text{run}} = \sqrt{\tau_{\text{eff}} T_{\text{ta}}}$	$T_{\text{run}} = \frac{\Delta N_{\text{max}} \tau_{\text{eff}}}{N_0}$	$T_{\text{run}} = \tau_{\text{eff}} \min \left[ \ln \left( \sqrt{1 + \phi_{\text{piv}}(0)^2} \right), \ln \left( \frac{T_{\text{ta}} + T_{\text{run}} + \tau_{\text{eff}}}{\tau_{\text{eff}}} \right) \right]$
average luminosity	$L_{\text{ave}} = \hat{L} \frac{\tau_{\text{eff}}}{(\tau_{\text{eff}}^{1/2} + T_{\text{ta}}^{1/2})^2}$	$L_{\text{ave}} = \frac{L_0}{1 + \frac{L_0 \sigma_{\text{rel}}^2 T_{\text{ta}}}{\Delta N_{\text{max}} N_b}}$	$L_{\text{ave}} = \frac{\tau_{\text{eff}}}{T_{\text{ta}} + T_{\text{run}}} \left( 1 - e^{-T_{\text{run}}/\tau_{\text{eff}}} \right)$

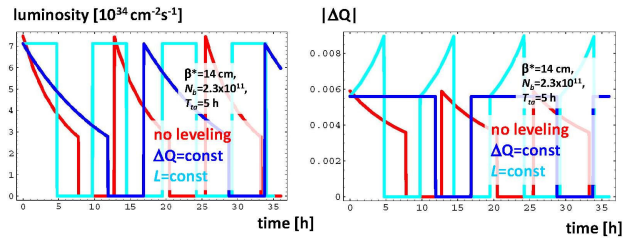


Figure 15: Example evolution of luminosity [left] and beam-beam tune shift [right] without leveling (red), leveling with constant luminosity (light blue), and with constant beam-beam tune shift (dark blue), considering a bunch intensity of  $N_b=2.3 \times 10^{11}$ ,  $\beta^*=14$  cm, and  $T_{\text{ta}}=5$  h.

Table 3: Example parameters without and with leveling for the scenario “phase 2+”.

	$\beta^*=14$ cm, 25 ns spacing, $T_{\text{ta}}=5$ h			
	no leveling	$L=\text{const}$	$\Delta Q_{\text{bb}}=\text{const}$	
$N_b(0)$ [ $10^{11}$ ]	2.3	2.3	2.3	2.3
$L(0)$ [ $10^{34} \text{cm}^{-2} \text{s}^{-1}$ ]	7.5	7.1	12.3	7.1
$ \Delta Q_{\text{bb}}(0) $	0.0059	0.0056	0.01	0.0056
$ \Delta Q_{\text{bb}}(T_{\text{run}}) $	0.0036	0.0090	0.01	0.0056
$\theta_c(0)$ [ $\mu\text{rad}$ ]	509	539	239	539
run time $T_{\text{run}}$ [h]	7.74	4.74	2.72	11.9
$\langle L \rangle$ [ $10^{34} \text{cm}^{-2} \text{s}^{-1}$ ]	2.8	3.5	3.6	3.2
events/#ing (0)	142	135	234	135

Table 4: Example parameters without and with leveling for the scenario of the 50-ns LPA scheme.

	$\beta^*=25$ cm, 50 ns spac., “LPA” $T_{\text{ta}}=5$ h		
	no leveling	$L=\text{const}$	$\Delta Q_{\text{bb}}=\text{const}$
$N_b(0)$ [ $10^{11}$ ]	4.2	4.2	4.2
$L(0)$ [ $10^{34} \text{cm}^{-2} \text{s}^{-1}$ ]	7.4	4.5	4.5
$ \Delta Q_{\text{bb}}(0) $	0.010	0.0056	0.0056
$ \Delta Q_{\text{bb}}(T_{\text{run}}) $	0.006	0.010	0.0056
$\theta_c(0)$ [ $\mu\text{rad}$ ]	381	672	672
run time $T_{\text{run}}$ [h]	7.45	6.0	23.2
$\langle L \rangle$ [ $10^{34} \text{cm}^{-2} \text{s}^{-1}$ ]	2.6	2.5	2.1
events/#ing (0)	280	172	172

## IMPACT OF TURNAROUND TIME

Figure 16 illustrates the impact of the turnaround time on the average luminosity, for several scenarios spanning the available parameter range. Reducing the turnaround time  $T_{\text{ta}}$  from 10 to 2 h increases the average luminosity  $\langle L \rangle$  by about a factor of 2, almost independently of the scenario. Overall the values of the average luminosity are rather similar for all 3 scenarios.

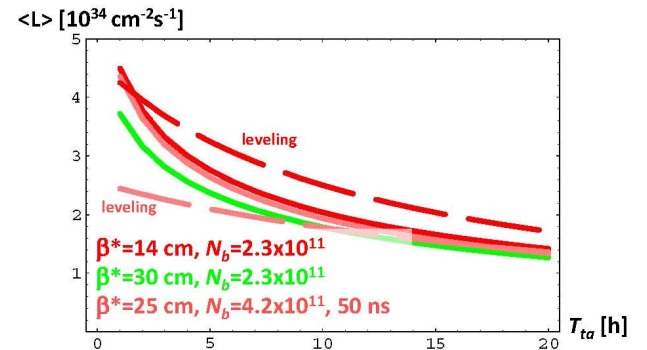


Figure 16: Dependence of the average luminosity on the turnaround time, for different values of  $\beta^*$ ,  $N_b$ , and bunch spacing, and without (solid lines) or with luminosity leveling (dashed). The “leveling” scheme assumed here results in a constant beam-beam tune shift.

## IMPACT OF BETA-STAR & INTENSITY

Figure 17 is the key plot of this paper. It illustrates the variation of the average luminosity with  $\beta^*$  and with the beam intensity, considering several upgrade scenarios. Evidently the beam intensity is much more important than  $\beta^*$ . Reducing  $\beta^*$  only raises the luminosity significantly if it is accompanied either by crab cavities [21] or by a smaller emittance [43]. The latter two measures have an identical effect on the average luminosity [43].

Figure 18 presents the transverse emittance needed to trace the curve for the reduced emittance scheme in Fig. 17. The emittance for the low-emittance scheme is determined so that the total tune shift does not exceed 0.01, while the long-range beam-beam separation is held constant equal to  $10\sigma$ .

$\langle L \rangle [10^{34} \text{ cm}^{-2} \text{ s}^{-1}]$

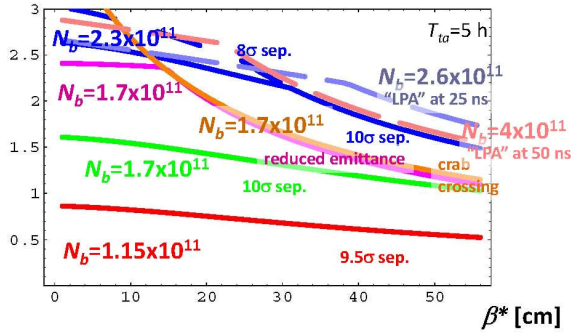


Figure 17: Average luminosity as a function of  $\beta^*$  for the nominal LHC and various upgrade scenarios with 25-ns and (one with) 50-ns bunch spacing, keeping the total beam-beam tune shift below or equal 0.01, and a long-range beam-beam separation of at least  $8\text{-}10\sigma$ . An average turnaround time of 5 h is assumed.

$\gamma\epsilon [\mu\text{m}]$

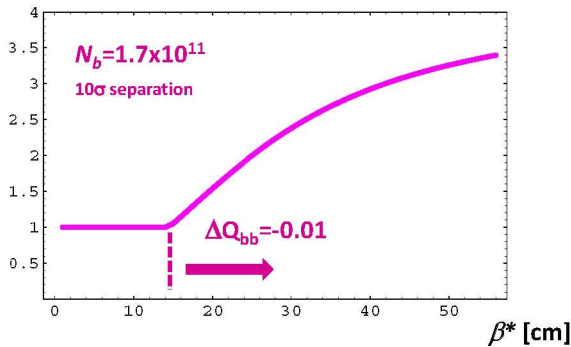


Figure 18: Emittance as a function of  $\beta^*$  for the reduced emittance scenario included in Fig. 17. For  $\beta^*$  values above 14 cm the emittance is adjusted so as to yield a constant beam-beam tune shift of 0.01. On the left side of the picture, for  $\beta^*$  values below 14 cm, it is assumed that the normalized rms emittance cannot be made smaller than  $1 \mu\text{m}$  ( $3.75 \mu\text{m}$  being the nominal value). The long-range separation is held constant, equal to  $10\sigma$ .

## CONCLUSIONS

Several upgrade scenarios are being proposed, with either 25 or 50-ns bunch spacing. For the parameter sets presented here, annual luminosities of up to  $150\text{-}300 \text{ fb}^{-1}$  could be expected, assuming a realistic run duration (200 days) and machine availability (60%).

Separate cryoplants for the IRs in LHC points 1, 5 and 4 are required for any LHC operation beyond the ultimate luminosity. The cooling capacity for the arc beam screen then limits the maximum bunch intensity to about  $N_b \sim 2.3 \times 10^{11}$  at 25-ns bunch spacing, and to about  $5.0 \times 10^{11}$  for 50-ns spacing.

Reducing the turnaround time from 10 to 2 h increases the average luminosity by about a factor of 2 in many of the scenarios. Reducing  $\beta^*$  by a factor 2 increases the average luminosity only by 10-20% unless the  $\beta^*$  reduction is accompanied by crab cavities or by a smaller transverse emittance. Increasing the bunch intensity from nominal to ultimate and to the limit set by the cooling loops is the most efficient way to increase the average luminosity. A factor 2 increase in the bunch population  $N_b$  translates into 3 times higher average luminosity! Crab crossing increases the average luminosity by between 10 and 100%, depending on  $\beta^*$  and bunch intensity.

Crab cavities would also allow for easy luminosity leveling and greatly expand the operational flexibility. Leveling with the (effective) crossing angle can increase the physics run time by a factor 1.5-3, and in addition reduce pile up by 30-40%, at constant average luminosity, or alternatively raise the average luminosity by  $\sim 15\%$ .

The present approach to luminosity optimization assumes collisions in two interaction points, ATLAS and CMS, though collisions for LHCb (or ALICE) could be provided in an almost transparent manner for the 50-ns scenario, through the addition of lower-intensity satellite bunches. An official policy or guideline for ALICE and LHCb running at the time of the ‘‘Super-LHC’’ would be desirable.

Future research should focus on understanding and mitigating other bunch-intensity limits, on minimizing the turnaround time, and on a new interaction-region design with (much) smaller  $\beta^*$  together with crab cavities and/or smaller-emittance beams.

## ACKNOWLEDGEMENTS

I would like to thank many colleagues and friends, who have - over the last decade - contributed ideas on the LHC upgrade, including R. Assmann, R. Bailey, C. Bhat, O. Brüning, R. Calaga, H. Damerou, D. Denegri, O. Dominguez, U. Dorda, L. Evans, S. Fartoukh, R. Garoby, M. Giovannozzi, B. Goddard, N. Hessey, B. Jeanneret, E. Jensen, J.-P. Koutchouk, H. Maury Cuna, S. Myers, J. Nash, M. Nessi, K. Ohmi, R. Ostojic, Y. Papaphilippou, L. Rossi, F. Ruggiero, G. Rumolo, W. Scandale, D. Schulte, E. Shaposhnikova, G. Sterbini, K. Takayama, L. Tavian, T. Taylor, E. Todesco, R. Tomas and E. Tsesmelis. I thank O. Brüning for comments on the paper.

## REFERENCES

- [1] O. Brüning et al., “LHC Luminosity and Energy Upgrade: A Feasibility Study,” CERN-LHC-Project-Report-626 (2002)
- [2] CARE-HHH network, web site <http://cern.ch/care-hhh>.
- [3] Proceedings of the 1st CARE-HHH-APD Workshop on *Beam Dynamics in Future Hadron Colliders and Rapidly Cycling High-Intensity Synchrotrons – ‘HHH 2004,’* CERN, Geneva, November 2004, edited by F. Ruggiero, W. Scandale, F. Zimmermann, CERN Yellow Report 2005-006.
- [4] Proceedings of the 3rd CARE-HHH-APD Workshop: *Towards a Roadmap for the Upgrade of the LHC and GSI Accelerator Complex – ‘LHC-LUMI-06,’* Valencia, Spain, October 2006, edited by W. Scandale, T. Taylor, F. Zimmermann, CERN Yellow Report 2007-002
- [5] Proceedings of the CARE-HHH-APD Workshop on Finalizing the Roadmap for the Upgrade of the CERN and GSI Accelerator Complex – ‘BEAM’07,’ BEAM’07, CERN, Geneva, October 2007, edited by W. Scandale, and F. Zimmermann, CERN Yellow Report 2008-005.
- [6] Proceedings of the Final CARE-HHH Workshop on *Scenarios for the LHC Upgrade and FAIR – ‘HHH-2008,’* Chavannes-de-Bogis, November 2008, edited by W. Scandale, and F. Zimmermann, CERN Yellow Report 2009-004.
- [7] EuCARD-AccNet network, web site <http://accnet.lal.in2p3.fr/>
- [8] S. Fartoukh, “Flat Beam Optics,” 19<sup>th</sup> Meeting of the LHC Machine Advisory Committee, 16 June 2006.
- [9] J. Gareyte, “Beam-Beam Design Criteria for LHC,” in Proceedings of the Workshop on *Beam-Beam Effects in Large Hadron Colliders – ‘LHC99,’* CERN, Geneva, April 1999, edited by J. Poole and F. Zimmermann, CERN-SL-99-039 AP.
- [10] H. Dijkstra, private communication, 11 March 2006
- [11] F. Zimmermann, “LHC Upgrade Plan and Ideas,” LHCb Upgrade Workshop Edinburgh, January 2007; <http://www.nesc.ac.uk/esi/events/729/>
- [12] F. Zimmermann, “Overview of LHC Machine Upgrade Plans from an LHCb Perspective,” LHCb Upgrade Meeting, CERN, 5 August 2008.
- [13] Y. Papaphilippou, F. Zimmermann, Phys.Rev.ST Accel.Beams 2:104001, 1999.
- [14] S. Fartoukh, “Optics Challenges and Solutions for the LHC Insertions Upgrade Phase I,” LHC Performance Workshop Chamonix 2010, these proceedings.
- [15] F. Ruggiero, F. Zimmermann, “Luminosity optimization near the beam-beam limit by increasing bunch length or crossing angle,” Phys.Rev.ST Accel.Beams 5:061001 (2002).
- [16] F. Ruggiero, G. Rumolo, F. Zimmermann, Y. Papaphilippou, “Beam dynamics studies for uniform (hollow) bunches or super-bunches in the LHC: Beam-beam effects, electron cloud, longitudinal dynamics, and intrabeam scattering,” LHC Project Report 627 (2002).
- [17] O. Brüning, “LHC Challenges and Performance Limitations,” SLAC Summer Institute, August 2009.
- [18] K. Cornelis, W. Herr, M. Meddahi, “Proton Antiproton Collisions at a Finite Crossing Angle in the SPS,” PAC’91 San Francisco (1991).
- [19] R. Palmer, “Energy Scaling, Crab Crossing and the Pair Problem,” DPF Summer Study Snowmass ’88: High Energy Physics in the 1990’s, Snowmass, Colo., Jun 27 - Jul 15, 1988, SLAC-PUB-4707 (1988).
- [20] K. Oide and K. Yokoya, “The Crab Crossing Scheme For Storage Ring Colliders,” Phys.Rev.A40:315-316 (1989).
- [21] Joint EuCARD-AccNet and US-LARP 3<sup>rd</sup> LHC Crab Cavity Workshop “LHC-CC09,” CERN, Geneva, 16-18 September 2009, workshop web site <http://indico.cern.ch/conferenceDisplay.py?confId=55309>
- [22] Discussions with L. Tavian and B. Jeanneret, early in 2005
- [23] F. Zimmermann, “Electron Cloud Update,” 17<sup>th</sup> Meeting of the LHC Machine Advisory Committee, 10 June 2005
- [24] L. Tavian, “Cryogenic Limits,” presentation at CARE-HHH LUMI’06 workshop, Valencia, Spain; <http://care-hhh.web.cern.ch/CARE-HHH/LUMI-06/>
- [25] H. Maury Cuna, “Study of the Heat Load due to the Electron Cloud in the LHC and in Higher-Luminosity LHC Extensions,” (in Spanish), Master Thesis U. Merida (and shortened English version), August 2009; available at <http://ab-abp-rlc.web.cern.ch/ab-abp-rlc-ecloud/>
- [26] F. Ruggiero, X. Zhang, “Collective instabilities in the LHC: Electron cloud and satellite bunches,” Workshop on instabilities of high intensity hadron beams in rings. AIP Conference Proceedings, Volume 496, pp. 40-48 (1999).
- [27] F. Zimmermann, “Electron-Cloud Simulations for SPS and LHC,” Proceedings of LEP and LHC Performance Workshop Chamonix X, January 2000, CERN-SL-2000-007 DI.
- [28] F. Ruggiero, “LHC beam parameters and IR upgrade options,” CARE-HHH LUMI’05 workshop, Arcidosso, Italy; workshop web site <http://care-hhh.web.cern.ch/CARE-HHH/LUMI-05>
- [29] R. Ostojic et al., “Conceptual Design of the LHC Interaction Region Upgrade: Phase-I,” LHC-PROJECT-Report-1163 (2008).
- [30] E. Todesco et al, “A Concept for the LHC luminosity upgrade based on strong beta\* reduction combined with a minimized geometrical luminosity loss factor,” PAC’07 Albuquerque (2007).
- [31] F. Zimmermann, “Optimum Run Time, Integrated Luminosity etc.,” ABP-RLC meeting 23.09.2005, <http://ab-abp-rlc.web.cern.ch/ab-abp-rlc/Meetings/2005/2005.09.23/lumilifetime-FZ.pdf>

- [32] Review of Particle Physics. Particle Data Group (C. Amsler et al.). Published in Phys. Lett. B667:1, 2008.
- [33] M. Lamont, "Comparison of integrated luminosities," Chamonix 2010, these proceedings.
- [34] O. Brüning et al., "LHC Design Report , v.1: the LHC Main Ring," CERN-2004-003-V-1, Chapter 20, Early Plans for Commissioning and Operation, Figure 20.1 (2004).
- [35] R. Schmidt, "The LHC – Operation and Machine Protection," CERN Academic Training March 2003.
- [36] O. Brüning, "Turnaround time in Modern Hadron Colliders & Store-Length Optimization," Proc. of CARE-HHH workshop BEAM'07, CERN, Geneva, October 2007, edited by W. Scandale, and F. Zimmermann, CERN Yellow Report 2008-005.
- [37] F. Zimmermann, "Luminosity Limitations at Hadron Colliders," Proc. 18th International Conference on High Energy Accelerators, Tsukuba, Japan, 26 - 30 March 2001
- [38] D. Brandt, "Review of the LHC Ion Programme," LHC Project Report 450 (2000).
- [39] F. Zimmermann, W. Scandale, "Two Scenarios for the LHC Luminosity Upgrade," PAF/POFPA Meeting, CERN, 13. February 2007; see <http://care-hhh.web.cern.ch/care-hhh/publications.htm>
- [40] G. Sterbini, J.P. Koutchouk, "A Luminosity Leveling Method for LHC Luminosity Upgrade using an Early Separation Scheme," LHC Project Note 403, May 2007.
- [41] J.-P. Koutchouk and G. Sterbini, "Luminosity Leveling with Angle," Proc. Of CARE-HHH-APD Workshop on Finalizing the Roadmap for the Upgrade of the CERN and GSI Accelerator Complex "Beam'07," CERN, Geneva, October 2007, CERN Yellow Report CERN-2008-005.
- [42] F. Zimmermann, W. Scandale, "LHC Machine Upgrade Parameters," Meeting on Machine-Experiment Interface Issues for the LHC Luminosity Upgrade, 24 July 2007
- [43] R. Garoby, "Potential of Reduced Transverse Emittances for Increasing the LHC Luminosity," in Proceedings of the Final CARE-HHH Workshop on *Scenarios for the LHC Upgrade and FAIR – 'HHH-2008,'* Chavannes-de-Bogis, November 2008, CERN Yellow Report 2009-004, pp. 21-22.